International Journal of Power Electronics and Drive System (IJPEDS)
Vol. 4, No. 2, June 2014, pp. 192~203
ISSN: 2088-8694

Control of Four Switch Three Phase Inverter Fed Induction Motor Drives Based Speed and Stator Resistance Estimation

M. K. Metwally
Departement of Electrical Engineering, Menoufiya University, Faculty of Engineering, Menoufiya, Egypt

Article Info

Article history:

Received Nov 4, 2013
Revised Jan 9, 2014
Accepted Jan 26, 2014

Keyword:

Induction motor
Four switch three phase inverter
Sensorless control
Model reference adaptive system (MRAS)
Stator resistance identification

ABSTRACT

This paper presents sensorless position and speed control for a four-switch three-phase inverter (FSTPI) fed induction motor drive. Accurate knowledge of stator resistance is of utmost importance for correct operation of a number of speed sensorless induction motor control schemes in the low speed region. Since stator resistance inevitably varies with operating conditions, stable and accurate operation at near-zero speed requires an appropriate identification algorithm for the stator resistance. The paper proposes such an identification algorithm, which is developed for the rotor flux based model reference adaptive system (MRAS) type of the speed estimator in conjunction with a rotor flux oriented control scheme. In this speed estimation method only one (out of the two available) degree of freedom is utilized for speed estimation. It is utilize the second available degree of freedom as a mean for adapting the stator resistance. The parallel stator resistance and rotor speed identification algorithm is developed in a systematic manner, using Popov's hyper stability theory. It increases the complexity of the overall control system insignificantly and enables correct speed estimation and stable drive operation at near-zero speeds. The proposed speed and position estimator with parallel stator resistance identification for FSTPI fed induction motor at very low speed under high load operation is verified by simulation and experimental results. The results show the robustness of the proposed method with FSTPI.

Corresponding Author:

M. K. Metwally
Departement of Electrical Engineering,
Menoufiya University,
Faculty of Engineering,
Menoufiya, Egypt.
Email: mohkamel2007@yahoo.com

1. INTRODUCTION

The induction motor has found very wide industrial applications due to its well-known advantages as simple construction, reliability and low cost. The most popular high performance induction motor control method is that one known as Field-Oriented Control. It is based on a *d-q* reference frame rotating synchronously with the rotor flux vector, which allows achieving a decoupled control between the flux and the produced torque, likewise to a separately excited DC motor [1].

In Direct Field-Oriented Control, both the instantaneous magnitude and position of the rotor flux vector are supposed to be precisely known. However, as the rotor flux cannot be directly measured, efforts have been made to estimate the rotor flux using various kinds of observers, based on the measurements of the stator currents, the stator voltages and the motor speed. An important problem is that the exact values of the motor parameters, from which the observer and some high performance control systems depend, are different from nominal values and change with respect to the temperature and the operating conditions. Another question is the need of a speed sensor to provide the rotor speed measurement, necessary to regulation

purpose as well as observer operation. The presence of this sensor increases the drive cost and can reduce the robustness of the overall system; moreover, in some cases a speed sensor cannot be mounted, such as motor drives in a hostile environment and very high speed motor drives.

The extended Kalman filters for simultaneous estimation of the rotor flux, the speed and some motor parameters (frequently only the rotor resistance, the parameter subjected to the widest variation) have been proposed as a potential solution to the above problems [2], [3]. Unfortunately, this approach has some inherent disadvantages, such as the influence of noise and computation burden.

In the last years, the sliding-mode observer has represented an attractive choice for its being quite robust to disturbances, parameter deviations and system noise [4], [5]. Adaptive flux sliding-mode observers, in which the motor speed is estimated by additional equations, have been designed trying to reduce the influence of parameters variations [6]-[8].

The stator resistance identification methods are by far the most frequently met and it includes all the estimators where an updated stator resistance value is obtained through an adaptive mechanism [9]-[19]. Proportional integral (PI) or integral (I) controllers are used for this purpose. In principle, two distinct sub-categories exist. In observer based systems [11]-[12], [15], [18]-[19] the error quantity, which serves as an input into the stator resistance adaptation mechanism, is determined with the difference between the measured and the observed stator current.

In MRAS based systems [9]-[10], [13]-[14], [16]-[17] the choice of the error quantity is more versatile. The scheme of [9] operates in the rotating reference frame and the error quantity is determined with the difference between the rotor flux d-axis components obtained from the voltage and current models. The method of [10] is similar, except that it utilizes the rotor flux reference and only one estimate of the rotor flux d-axis component information of the error quantity. The error quantity in [13] is based on active power, while the one in [14] is obtained as a sum of the products of rotor current and rotor flux d-q axis components. The error signal of [17] utilizes an error in the stator d-axis current component as the input of the integral controller, while the error quantity of [18] is formed in such a way that the stator resistance identification is independent of the total leakage inductance. From the point of view of the method of stator resistance identification proposed in this paper, especially relevant are the MRAS schemes of [9]-[10], [16], as discussed shortly.

This paper presents a model reference adaptive system working in parallel with a particular adaptive scheme. This scheme is able to estimate either the motor resistive parameters or the rotor speed. Thus, the MRAS allow obtaining robust rotor flux estimation. Moreover, the configuration with the adaptive scheme for the estimation of stator resistance value allows to implement high accurate speed controls, where there is the need to have constantly the right values of these parameters to preserve high level performances. On the other hand, the configuration with the rotor speed estimation can be used for the implementation of a sensorless control. Finally, the validity of the proposed algorithms is verified by means of simulation and experimental results.

2. SENSORLESS VECTOR CONTROL

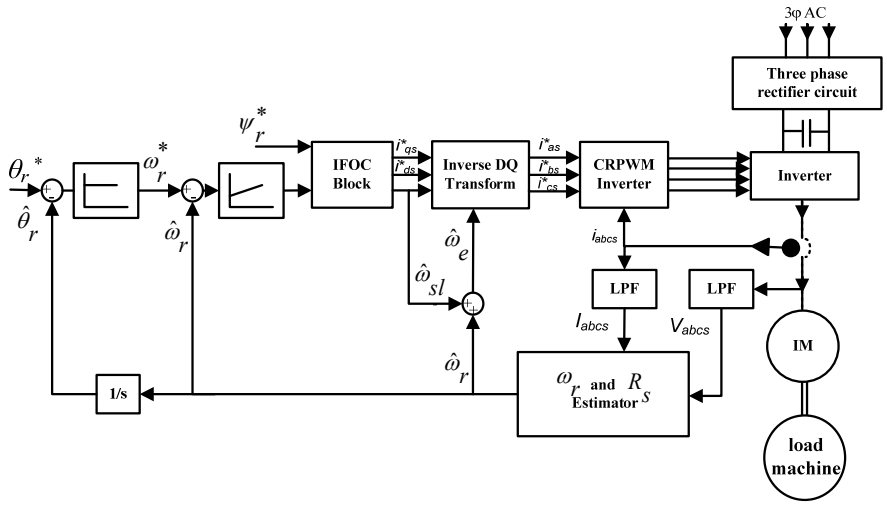

Figure 1. Block diagram of sensorless vector control

Vector control is a method that separates the flux and torque currents so as to linearly control the output torque of an induction motor. As such, vector control requires precise knowledge of the angle of rotor flux. Normally, with vector control, the angle of rotor flux is indirectly estimated using the motor speed measured from a speed sensor attached to the rotor shaft. Although a vector controller using a speed sensor can accurately control a servo system, various problems occurs as a result of the speed sensor. Therefore, sensorless vector control, which can control the torque without a speed sensor, has become an important research topic.

Although many methods have already been proposed for speed estimation, the MRAS approach is the most attractive method because in this method, the models are simple and very easy to implement [20]. Figure 1 shows a block diagram of a sensorless vector controller where estimated speed is used for the vector control. The control scheme of induction motor drive consists of the modeling of the inverter, sensorless control algorithm and the overall system controller, which are discussed in the following subsections.

2.1. FSTPI Topology And Space Vector Analysis

The FSTPI topology consists of 4 power switches that provide two of the inverter output phases. The third phase is fed by the dc link from the center of a split-capacitor bank, as shown in Figure 2

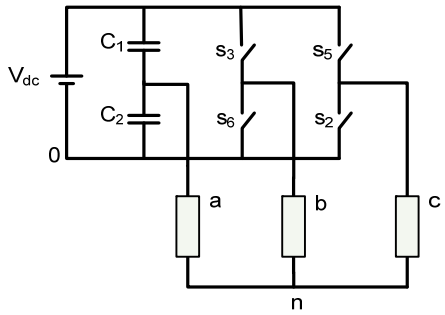

Figure 2. Power Circuit of 4-switch 3-phase inverter

With respect to the circuit of Figure 2**,** the phase voltages at the 3-phase load terminals depend on the conducting states of the power switches. The calculations of phase voltages are presented in Table 1.

Table 1. The values of Line-zero & Line-neutral load voltages in FSTPI

Switch on		Vector	V_{bo}	V_{co}	V_{an}	V_{bn}	V_{cn}
3	5	1 1	V_{dc}	V_{dc}	$-V_{dc}/3$	$V_{dc}/6$	$V_{dc}/6$
6	2	0 0	0	0	$V_{dc}/3$	$-V_{dc}/6$	$-V_{dc}/6$
3	2	1 0	V_{dc}	0	0	$V_{dc}/2$	$-V_{dc}/2$
5	6	0 1	0	V_{dc}	0	$-V_{dc}/2$	$V_{dc}/2$

The resultant space vector of the inverter output voltage is calculated using the following equations:

$$\underline{V}_s = \frac{2}{3}\left[V_{an} + aV_{an} + a^2 V_{cn}\right] \quad (1)$$

$$\underline{V}_s = V_d + jV_q \quad (2)$$

The voltage space vector can be computed with the aid of the gating signals S3 and S5:

$$\underline{V}_s = \frac{2}{3}V_{dc}\left[0.5 + aS_3 + a^2 S_5\right] \quad (3)$$

Where a=$e^{j2\pi/3}$

Thus, the orthogonal components V_d and V_q are:

$$V_d = \frac{1}{3}V_{dc}(1 - S_3 - S_5) \tag{4}$$

$$V_q = \frac{1}{\sqrt{3}}V_{dc}(S_3 - S_5) \tag{5}$$

The numerical calculation of the V_d and V_q, leads to the following important facts:

a) The discrete voltage space vector has four active vectors (unlike the six switch three phase inverter (SSTPI) which has 6-active vectors with equal magnitude).
b) These vectors have unequal magnitudes.
c) No zero vectors are found (unlike the SSTPI inverter that has 2-zero vectors).

Figure 3 shows the equivalent discrete voltage space vector of the FSTPI topology.

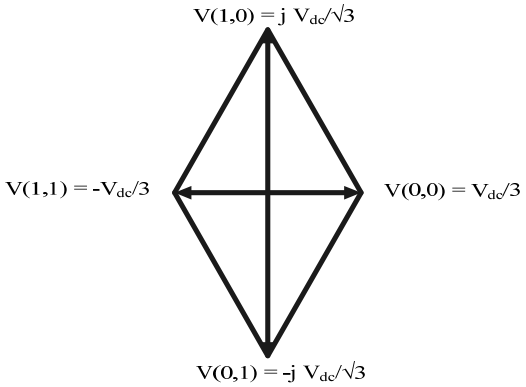

Figure 3. Equivalent active voltage vectors of (FSTPI)

2.2. Speed Estimation Scheme Based on MRAS

The speed estimator, analyzed in this paper, is the one originally proposed in [21] and illustrated in Figure 4, where the two left-hand side blocks perform integration of Equation (6) and (7). It relies on measured stator currents and measured stator voltages and is composed of the reference (voltage) and the adjustable (current) model. The estimator operates in the stationary reference frame (α, β) and it is described with the following equations [21]:

$$p\hat{\underline{\psi}}^s_{rV} = \frac{L_r}{L_m}\left[\underline{u}^s_s - (\hat{R}_s + \sigma L_s p)\underline{i}^s_s\right] \tag{6}$$

$$p\hat{\underline{\psi}}^s_{rI} = \frac{L_m}{T_r}\underline{i}^s_s - \left[\frac{1}{T_r} - j\hat{\omega}\right]\hat{\underline{\psi}}^s_{rI} \tag{7}$$

$$\hat{\omega} = \left[K_{p\omega} + \frac{K_{I\omega}}{p}\right]e_\omega \tag{8}$$

$$e_\omega = \hat{\underline{\psi}}^s_{rI} \times \hat{\underline{\psi}}^s_{rV} = \hat{\underline{\psi}}_{\alpha rI}\hat{\underline{\psi}}_{\beta rV} - \hat{\underline{\psi}}_{\beta rI}\hat{\underline{\psi}}_{\alpha rV} \tag{9}$$

A hat above a symbol in (6)-(9) denotes estimated quantities, symbol *p* stands for *d*/*dt*, *Tr* is the rotor time constant and $\sigma = 1 - L_m^2/(L_s L_r)$. All the parameters in the motor and the estimator are assumed to

be of the same value, except for the stator resistance (hence a hat above the symbol in (6)). Underlined variables are space vectors, and sub-scripts *V* and *I* stand for the outputs of the voltage (reference) and current (adjustable) models, respectively. Voltage, current and flux are denoted with *u*, *i* and ψ, respectively, and subscripts *s* and *r* stand for stator and rotor, respectively. Superscript *s* in space vector symbols denotes the stationary reference frame.

As is evident from (6)-(9) and Figure 4, the adaptive mechanism (PI controller) relies on an error quantity that represents the difference between the instantaneous positions of the two rotor flux estimates. The second degree of freedom, the difference in amplitudes of the two rotor flux estimates, is not utilized. The parallel rotor speed and stator resistance MRAS estimation scheme, which will be developed in the next section, will make use of this second degree of freedom to achieve simultaneous estimation of the two quantities. The role of the reference and the adjustable model will be interchanged for this purpose, since the rotor flux estimate of (7) is independent of stator resistance.

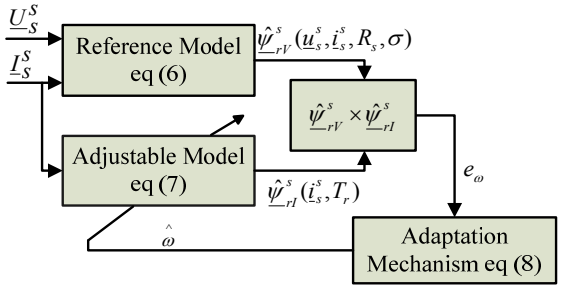

Figure 4. Basic configuration of the rotor flux based on MRAS speed estimator

2.3. Parallel Rotor Speed and Stator Resistance estimation

Parallel rotor speed and stator resistance estimation scheme is based on the concept of hyperstability [21] in order to make the system asymptotically stable. For the purpose of deriving an adaptation mechanism it is valid to initially treat rotor speed as a constant parameter, since it changes slowly compared to the change in rotor flux. The stator resistance of the motor varies with temperature, but variations are slow so that it can be treated as a constant parameter, too. The configuration of the parallel rotor speed and stator resistance is shown in Figure 5 and is discussed in detail next. Let *Rs* and ω denote the true values of the stator resistance in the motor and rotor speed, respectively. These are in general different from the estimated values. Consequently, a mismatch between the estimated and true rotor flux space vectors appears as well. The error equations for the voltage and the current model outputs can then be written as:

$$p\underline{\varepsilon}_V = -\frac{L_r}{L_m}(R_s - \hat{R}_s)\underline{i}_s^s \tag{10a}$$

$$\underline{\varepsilon}_V = \underline{\psi}_{rV}^s - \hat{\underline{\psi}}_{rV}^s = \varepsilon_{\alpha V} + j\varepsilon_{\beta V} \tag{10b}$$

$$p\underline{\varepsilon}_I = \left(j\omega - \frac{1}{T_r}\right)\underline{\varepsilon}_I + j(\omega - \hat{\omega})\hat{\underline{\psi}}_{rI}^s \tag{11a}$$

$$\underline{\varepsilon}_I = \underline{\psi}_{rI}^s - \hat{\underline{\psi}}_{rI}^s = \varepsilon_{\alpha I} + j\varepsilon_{\beta I} \tag{11b}$$

Symbols $\underline{\psi}_{rV}^s$, $\underline{\psi}_{rI}^s$ in (10b), (11b) stand for true values of the two rotor flux space vectors.

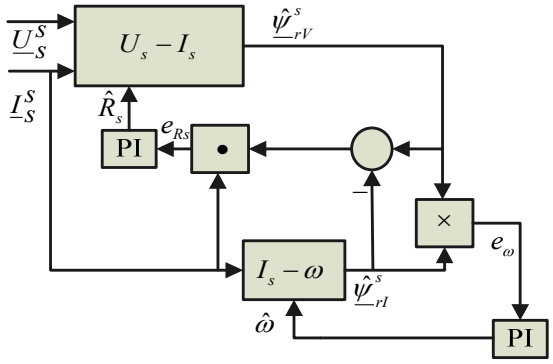

Figure 5. Structure of the MRAS system of parallel rotor speed and stator resistance estimation

The system is hyper-stable if the input and output of nonlinear block satisfy Popov's criterion [21]. The adaptive mechanism for rotor speed estimation and stator resistance identification is given in (12), (13) respectively.

$$\hat{\omega} = \left(K_{p\omega} + \frac{k_{I\omega}}{p} \right) \left(\underline{\varepsilon}_I^T J \hat{\underline{\psi}}_{rI}^s \right) = \left(K_{p\omega} + \frac{k_{I\omega}}{p} \right) e_\omega \tag{12}$$

$$J = \begin{bmatrix} 0 & -1 \\ 1 & 0 \end{bmatrix}$$

$$\hat{R}_s = \left(K_{pR_s} + \frac{k_{IR_s}}{p} \right) \left(-\underline{\varepsilon}_V^T i_s \right) = \left(K_{pR_s} + \frac{k_{IR_s}}{p} \right) e_{R_s} \tag{13}$$

Where $k_{p\omega}$, $k_{I\omega}$, $k_{pRs,}$ k_{IRs}, are PI controller parameters of rotor speed and stator resistance adaptation mechanisms respectively. The role of the reference and the adjustable models is interchangeable in the parallel system of rotor speed and stator resistance estimation. The speed and stator resistance can be estimated in parallel using (12), (13) at any speed. The rotor speed adaptation mechanism (12) is the same as in the customary MRAS speed estimator reviewed in Section B. Stator resistance adaptation mechanism (13) is, at the first sight, similar to the one of [9], [10]. However, stator resistance is here estimated in the stationary reference frame (rather than in the rotor flux oriented reference frame), and error quantity is obtained using two rotor flux space vector estimates (rather than the reference and a single estimated value, as in [10]). Further, stator resistance and rotor speed estimation operate in parallel, rather than sequentially as in [16]. This is enabled by utilizing the second available degree of freedom (the difference in rotor flux amplitudes) in the process of stator resistance estimation.

3. SIMULATION RESULTS

The proposed method was verified by SIMULINK/ MATLAB Program. The parameters of the induction motor used in the simulation are in appendix I. In all simulations, the estimated speed was used for vector controller and presented with the actual speed for comparison purpose.

Figure 6 shows the position waveforms when the sensorless position control was performed using the proposed method for FSTPI. The position change from 50° to 100° at t=2.5sec and then back to 50° at =4sec. The position command applied in the position controller is shown in Figure 6 upper diagram (blue) in degrees the estimated angle (red) and the actual rotor angle (black). The load torque is changed from 0 to 100% rated at t=1.5sec as shown in Figure 6 lower diagram. The results show the robustness of the sensorless position control during load change and position change operations.

Figure 7 shows the actual motor speed and estimated speed during load change and position change operation (upper diagram) and (lower diagram) shows the three phase motor currents during the same operation.

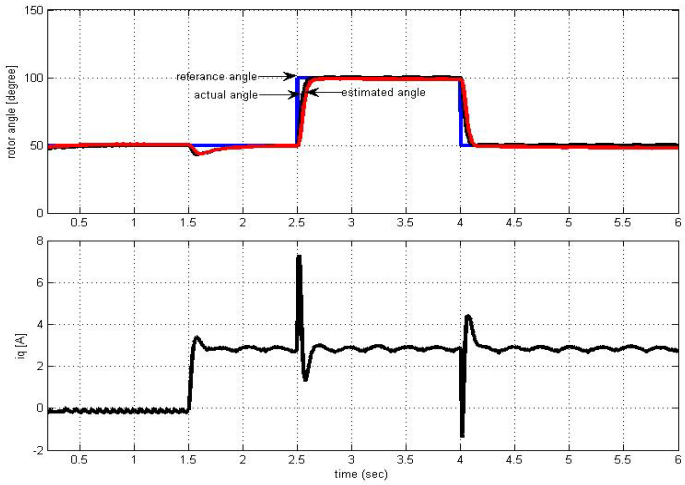

Figure 6. Upper: Reference (blue), estimated (red) and actual (black) rotor angles in °, Lower: torque current iq (A)

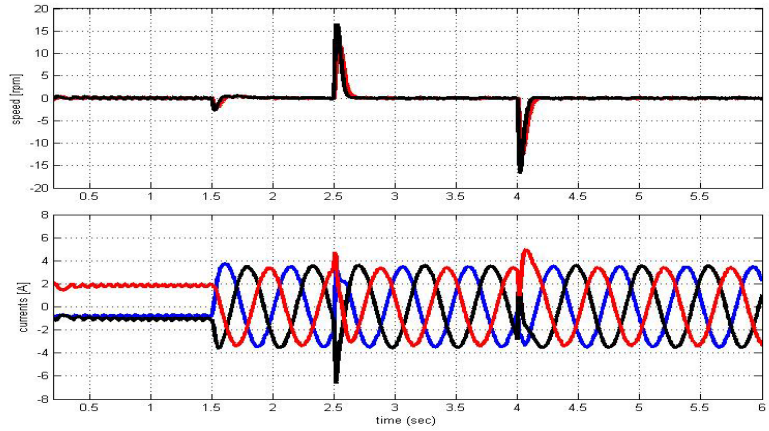

Figure 7. Upper: Actual speed (black) and estimated speed (red) in (rpm), Lower: motor currents Iabc in (A)

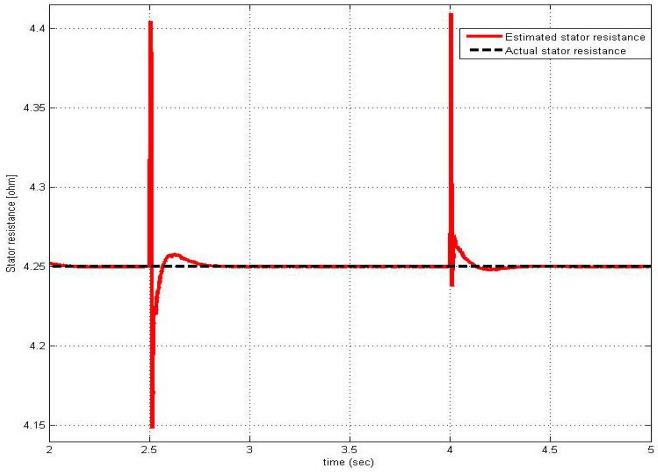

Figure 8. Actual stator resistance (black) and estimated stator resistance (red) in ohm

Figure 8 shows the actual stator resistance and the estimated resistance using the proposed estimation algorithm during the tests depicted in Figure 6 in ohm values the figure show the accuracy of the estimation algorithm during load and position change operations.

Figure 9 shows the speed waveforms when the sensorless speed control was performed at very low speed operation. The speed change from 5rpm to 50rpm at t=5sec. The speed command applied in the speed controller is shown in Figure 9 upper diagram (red) in rpm the estimated speed (blue) and the actual rotor speed (black). The load torque is changed from 0 to 90% rated at t=2sec as shown in Figure 9 lower diagram. The results show the robustness of the sensorless speed control during load change and speed change operations at very low speed.

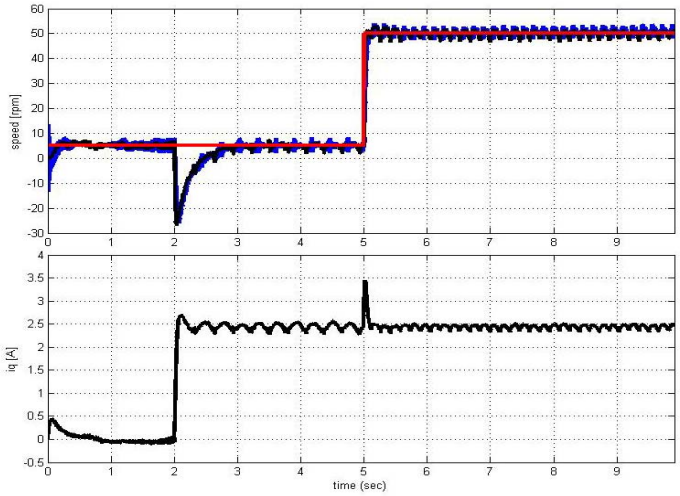

Figure 9. Upper: Reference (red), estimated (blue) and actual (black) rotor speeds in rpm, Lower: torque current iq (A)

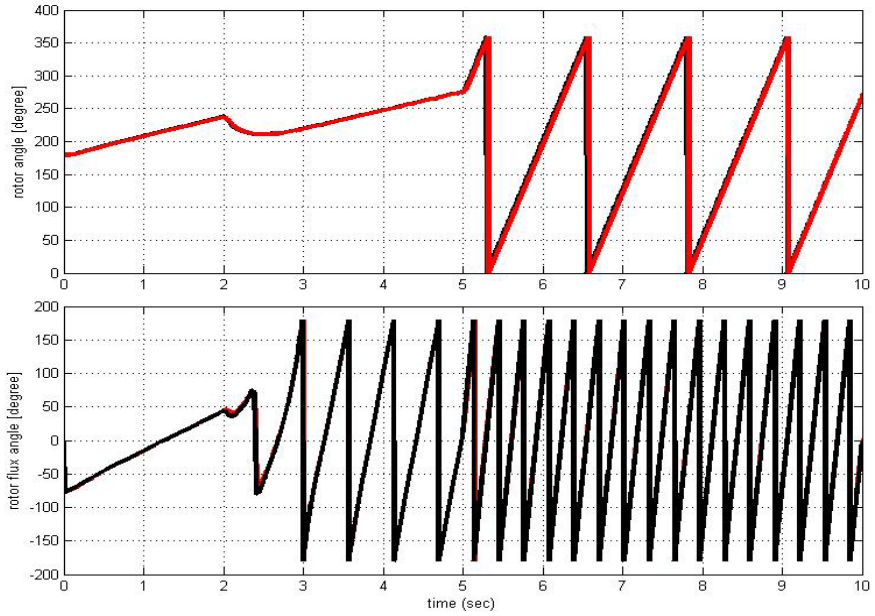

Figure 10. Upper: Actual rotor angle (black) and estimated rotor angle (red) in °, Lower: Actual rotor flux angle (black) and estimated rotor flux angle (red) in °

Figure 10 (upper diagram) shows the actual rotor angle (black) and estimate rotor angle (red) during load and speed change at very low speed operations also the actual rotor flux angle (black) and estimated

rotor flux angle (red) are shown in (lower diagram). The actual and estimated angle are coincidence to each other where the error is approximately zero during load change and speed operations which ensure the effectiveness of the proposed method at very low speeds.

Figure 11 shows the motor current in the stationary reference frame (α,β) (upper diagram) and the three phase motor currents Iabc (lower diagram).

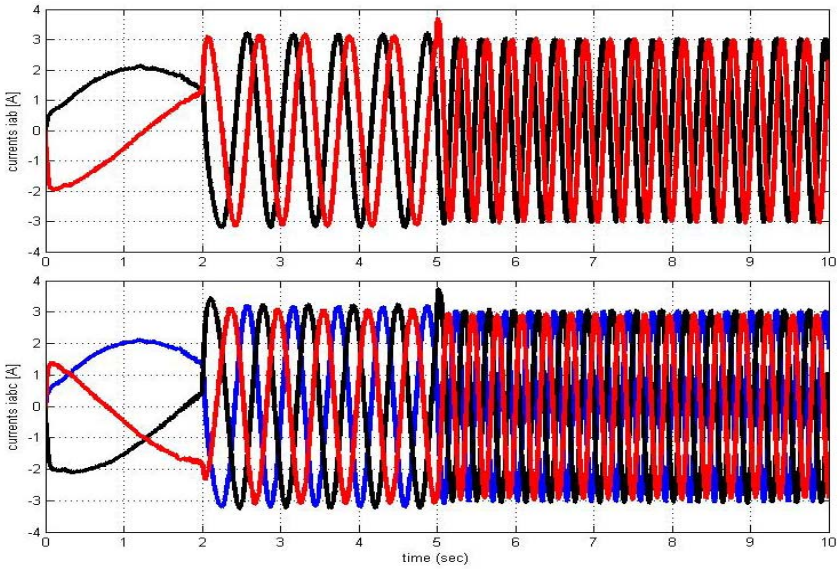

Figure 11. Upper: motor current in stationary reference frame (αβ) in (A), Lower: motor currents Iabc in (A)

4. EXPERIMENTAL RESULTS

The experimental setup is carried out by a DSpace 1103 system with I/O card for real time control (sampling time: Ts= 5e-5). An interface board was build to receive the gate-drive signal, isolated them and connected to the four switches which were implemented using integrated IGBT 100A. The output from FSTPI was connected to a three phase induction motor. The experimental results shown are from the IM drive coupled to a separately excited DC generator works as a load as shown in Figure 12. The machine was operated under sensorless position and speed control algorithm. The torque is applied by the DC generator under torque controlled mode. An optional position signal is available from an encoder with 1024 pulses per revolution.

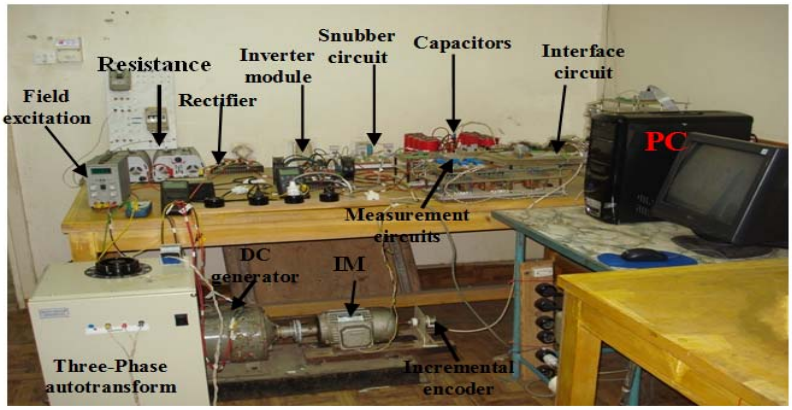

Figure 12. Experimental Setup

Figure 13 shows the dynamic behaviour of sensorless position control at 60% rated load with change in position of ± pi/3 rad. The deviation between actual and estimated rotor position is about ±1°

mechanical during transient position change and zero in steady state as shown in the lower diagram. The response time is limited by the bandwidth of the speed controller. The position controller is proportional only. Good performance of the system is achieved noting the current controller limitation to about 100% load current imposed by the inverter as shown in the middle diagram of Figure 15. It should be noted that the results presented indicate the potential of the method in combination with the signal processing.

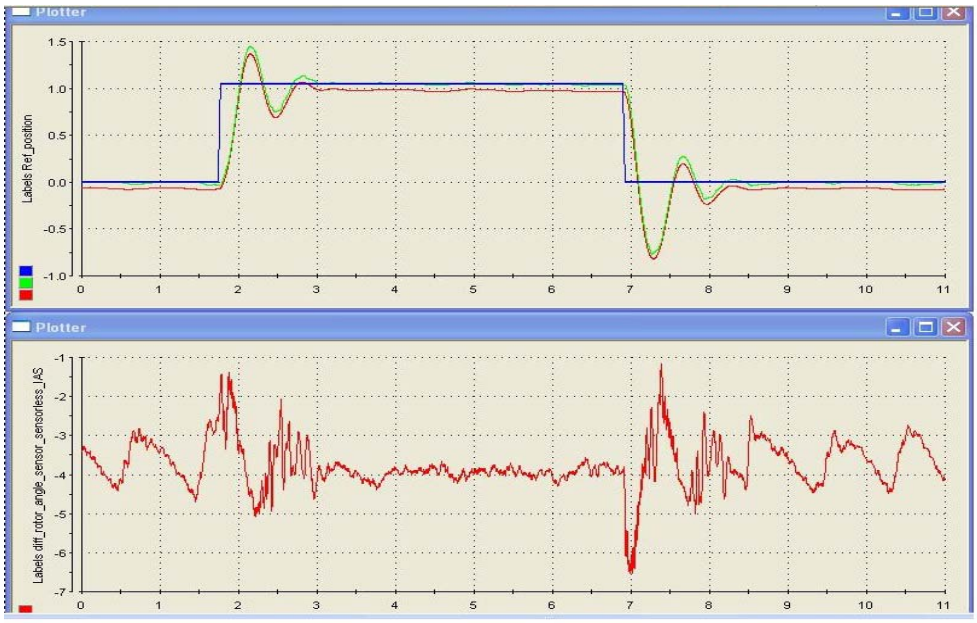

Figure 13. Sensorless position control at 60% load and change in position of ± pi/3 rad.Upper: Reference rotor angle (blue), estimated rotor angle (green), and actual rotor angle (red); Lower: error between actual and estimated rotor angles in (°)

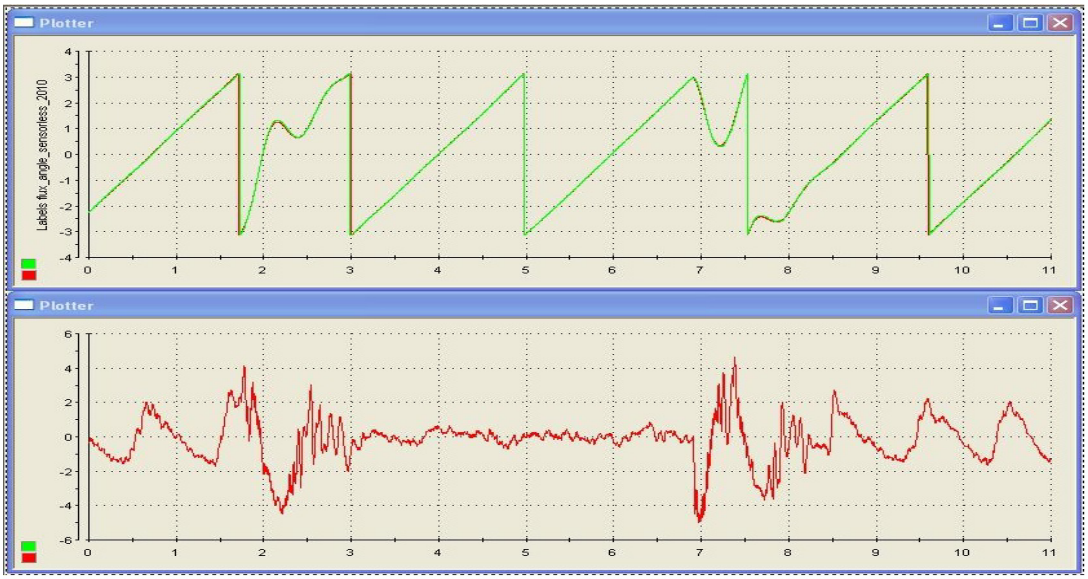

Figure 14. Upper: Reference flux angle (sensor-based) (red), and estimated sensorless flux angle (green), Lower: error between reference and estimated angles (°)

Figure 14 upper diagram shows the comparison between the actual rotor flux angle (red) and estimated rotor flux angle (green) during the test depicted in Figure 13 the error between the two angle is shown in lower diagram ± 2 degrees which confirm the effectiveness of the used control method.

Figure 15 upper diagram shows the αβ motor currents, middle diagram shows the load torque current Iq in (pu), as well as the motor speed (red) and sensorless estimated speed (green) is shown in lower diagram these results are captured during the test depicted in Figure 13.

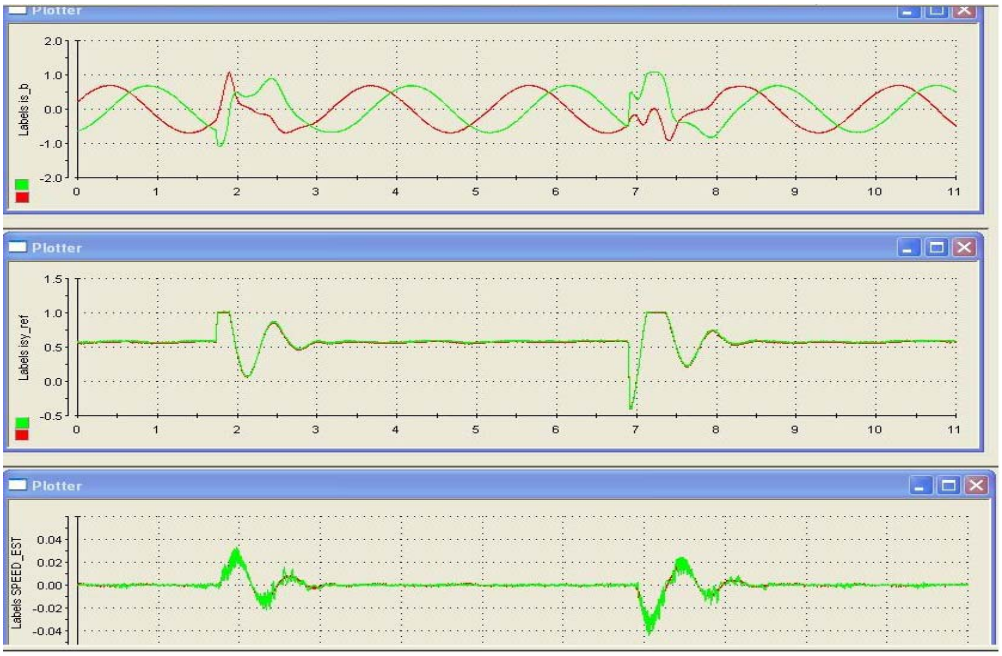

Figure 15. Upper: stator currents in αβ reference frame (pu), Middle: torque current component Iq (pu), Lower: actual speed (red) and estimated sensorless speed (green) in (pu)

5. CONCLUSION

The sensorless speed and position control using FSTPI fed induction motor drives was presented. It is based on parallel operation of MRAS and stator resistance identification schemes. The mathematical description of MRAS for rotor speed estimation in parallel with stator resistance identification is presented. The FSTP inverter fed IM drive system reduces the cost of the inverter, the switching losses and the complexity of the control algorithms as compared with the conventional SSTP inverter based drive. The vector control scheme has been incorporated in the integrated drive system to achieve high performance. A comparison between the actual stator resistance and estimated resistance is also presented during high load operation to show the validity of the identification algorithm. The FSTPI fed IM drive has been ensured robust and acceptable for low-cost applications such as automotive and home appliance. The simulation and experimental results verified the robustness of the FSTPI approach during sensorless position change under high load operation. The effectiveness of the used method at very low speed near zero speed under load operation is also presented.

REFERENCES

[1] P Vas. Sensorless Vector and Direct Torque Control, Clarendon Press, Oxford. 1998.
[2] D Sleeva Reddy, K Ankalamma, M Vijaya Kumar. A Comparison of Extended and Unscented Kalman Filters for the State Estimation of Induction Motor Drives. *International Journal of Engineering Research & Technology (IJERT)*. 2012; 1(7): 1-8.
[3] Yin, Zhong-gang, Zhao C, Zhong Yan-Ru, Liu J. Research on Robust Performance of Speed-Sensorless Vector Control for Induction Motor Using Interfacing Multiple-Model Extended Kalman Filter. *IEEE Transactions on Power Electronics*. 2013.
[4] Lin FJ, Hung YC, Chen SY. Field-programmable gate array-based intelligent dynamic sliding-mode control using recurrent wavelet neural network for linear ultrasonic motor. *IET Control Theory and Applications journal*. 2010.
[5] Yang Jie, Wang Qing-Lin, Li Yuan. *Sliding mode variable structure control theory: A survey*. Proceedings of control conference Chinese. 2012.
[6] Picardi C, Scibilia F. Sliding-Mode Observer with Resistances or Speed Adaptation for Field-Oriented Induction Motor Drives. *IEEE Industrial Electronics, IECON*. 2006: 1481-1486.

[7] M Tursini, R Petrella, F Parasiliti. Adaptive Sliding-Mode Observer for Sensorless Control of Induction Motors. *IEEE Trans. Ind. Applic.*, 2000; 36(5): 1380-1387.
[8] J Li, L Xu, Z Zhang. *An Adaptive Sliding Mode Observer for Induction Motor Sensorless Speed Control.* Ind. Appl. Conf., 39th Annual Meeting Conference. 2004: 1329-1334.
[9] M Tsuji, S Chen, K Izumi, E Yamada. A sensorless vector control system for induction motors using q-axis flux with stator resistance identification. *IEEE Trans. on Industrial Electronics.* 2001; 48(1): 185-194.
[10] K katsu, A Kawamura. Sensorless very low-speed and zero-speed estimations with online rotor resistance estimation of induction motor without signal injection. *IEEE Trans. on Industry Applications*. 2000; 36(3): 764-771.
[11] R Marino, S Peresada, P Tomei. On-line stator and rotor resistance estimation for induction motors. *IEEE Trans. on Control Systems Technology*. 2000; 8(3): 570-579.
[12] G Guidi, H Umida. A novel stator resistance estimation method for speed-sensorless induction motor drives. *IEEE Trans. on Industry Applications*. 36(6): 1619-1627, 2000.
[13] Zakaria MS El-Barbary, HZ Azazi, MK Metwally. Total Harmonic Distortion Analysis of a Four Switch 3-Phase Inverter Fed Speed Sensorless Control of IM Drives. *International Journal of Power Electronics and Drive Systems (IJPEDS).* 2014; 4(1).
[14] ED Mitronikas, AN Safacas, EC Tatakis. A new stator resistance tuning method for stator-flux-oriented vector-controlled induction motor drive. *IEEE Trans. on Industrial Electronics.* 2001; 48(6): 1148-1157.
[15] HZ Azazi, MK Metwally, ZS Elbarbary. A Cost Effective sensorless vector control of 4-Switch 3-Phase Inverter Fed IM using MRAS. *International Journal of Power Electronics and Drive Systems (IJPEDS)*. 2011; 1(2).
[16] MK Metwally. Sensorless Speed Control of 4- Switch Three Phase Inverter Fed Induction Motor Drives at Very Low and Zero Speed. *Alexandria Engineering Journal.* 2013.
[17] K Jarray, M Boussak, M Tholomier. *Stator resistance tuning in sensorless stator-flux field-oriented induction motor drive*. Proc. Int. Conf. on Electrical Machines ICEM. 2000; 543-547.
[18] B Raison, J Arza, G Rostaing, JP Rognon. *Comparison of two extended observers for the resistance estimation of an induction machine*. Proc. IEEE Ind. Appl. Soc. Annual Meeting IAS. 2000; 32(06).
[19] T Hamajima, M Hasegawa, S Doki, S Okuma. *Sensorless vector control of induction motor with stator resistance identification based on augmented error*. Proc. Power Conversion Conf., 2002; 504-509.
[20] MN Marwali, A Keyhani. *A comparative study of rotor flux MRAS and back EMF based MRAS speed estimators for speed sensorless vector control of induction machines*, in: Proceedings of the *IEEE-IAS Annual Meeting*. 1997: 160 166.
[21] Depenbrock M, Evers C. Model-based speed identification for induction Machines in the whole operating range. *IEEE Trans. On Industry electronics*. 2006; 53(1): 31-40.

APPENDIX I
The parameters of applied induction machine

Rated power	1 kw
Rated load torque	6.4 N.m.
No. of poles	4
Stator resistance	4.25 ohm
Rotor resistance	2.6840 ohm
Rotor leakage inductance	0.0221 H
Stator leakage inductance	0.0221 H
Mutual inductance	0.4114 H
Supply frequency	50 Hz
Motor speed	1500 r.p.m.
Supply voltage	380 volts
Inertia	0.018 kg.m^2

BIOGRAPHY OF AUTHOR

Dr. M. K. Metwally: received his doctoral degree in electrical engineering from Vienna University of Technology, Austria in March 2009. He is a lecturer in the Department of Electrical Engineering, Minoufiya University, Egypt.
His research interests cover AC machines control, the transient excitation of AC machines, sensorless control techniques, and signals processing.